DIGITAL ACCESS TO SCHOLARSHIP AT HARVARD

Citation	Krich, Jacob Jonathan, and Alán Aspuru-Guzik. 2011. Scaling and localization lengths of a topologically disordered system. Physical Review Letters 106(15): 156405.
Published Version	doi:10.1103/PhysRevLett.106.156405
Accessed	February 19, 2015 9:28:02 AM EST
Citable Link	http://nrs.harvard.edu/urn-3:HUL.InstRepos:8404293
Terms of Use	This article was downloaded from Harvard University's DASH repository, and is made available under the terms and conditions applicable to Open Access Policy Articles, as set forth at http://nrs.harvard.edu/urn-3:HUL.InstRepos:dash.current.terms-of-use#OAP

(Article begins on next page)

Scaling and localization lengths of a topologically disordered system

Jacob J. Krich[1, 2] and Alán Aspuru-Guzik[2]

[1] *Harvard University Center for the Environment, Cambridge, MA 02138*
[2] *Department of Chemistry and Chemical Biology, Harvard University, Cambridge, MA 02138*

We consider a noninteracting disordered system designed to model particle diffusion, relaxation in glasses, and impurity bands of semiconductors. Disorder originates in the random spatial distribution of sites. We find strong numerical evidence that this model displays the same universal behavior as the standard Anderson model. We use finite-size-scaling to find the localization length as a function of energy and density, including localized states away from the delocalization transition. Results at many energies all fit onto the same universal scaling curve.

The disorder-induced transition from extended to localized states in noninteracting quantum systems has been a rich source of physics insight for over 50 years [1]. It is relevant for a broad range of transport properties [2], glass formation [3], conductivity of composites [4], and random walks [5], as well as for nonradiative recombination in intermediate-band photovoltaics [6]. Scanning-tunneling and Bose-Einstein condensate experiments are increasingly able to probe localization properties directly [7]. The delocalization transition is usually studied by using the standard Anderson model, which considers a noninteracting tight-binding lattice with uniform nearest-neighbor coupling and random on-site energies [1]. For systems in which the disorder originates in the random configuration of the sites rather than, e.g., random local fields, it is better to consider the so-called topologically disordered or Lifshitz model, in which sites are distributed randomly in space; there are no on-site energies and all pairs of sites are connected by hopping terms with amplitude exponentially decaying with the distance between them [8]. As the density of sites increases, a localization/delocalization transition occurs, just as in the standard Anderson model. The density of states [3, 8–13] and localization properties [3, 10, 14] of this model have received much attention. Here we obtain the localization lengths of this model quantitatively as a function of wave function energy and site density. We adapt the finite-size scaling method, which has been successfully applied to the standard Anderson model [15–22], and give strong numerical evidence that this topologically disordered model displays the same universal behavior.

Model We consider noninteracting particles confined to identical lattice sites distributed randomly in space, with density ρ'. Particles can hop between sites with an exponentially decaying hopping coefficient. The Hamiltonian is

$$H = -\frac{V_0}{2} \sum_{n \neq m} e^{-r_{nm}/a_B^*} |n\rangle \langle m| \qquad (1)$$

where $|n\rangle$ are the site wave functions, r_{nm} is the distance between sites n and m, a_B^* is an effective Bohr radius

giving the decay of the wave functions, V_0 is an overall energy scale, and the sum runs over all pairs of sites. This model is called topologically disordered because there is no ordered structure describing which lattice sites are strongly coupled to each other. This model can describe the Hamiltonian of impurities with hydrogenic wave functions in a semiconductor, where the hopping originates in overlaps of their effective atomic wave functions. The dimensionless density is $\rho \equiv \rho' a_B^{*3}$. Experimentally, such systems are found to have a metal-insulator transition at $\rho^{1/3} \approx 0.26$ [23]. If the diagonal components of H are set such that each column sums to zero, the model can describe glass dynamics [3, 13] and continuous time quantum walks [5], but many properties are similar.

Localization lengths from quasi-1D scaling The localization length λ of a localized eigenstate is determined by the asymptotic decay of the wave function $\psi \sim e^{-|\boldsymbol{r}-\boldsymbol{r}_0|/\lambda}$, where $\boldsymbol{r}_0$ is some location of high wave function amplitude. Our goal is to find the localization length as a function of ρ and E. Finite-size scaling techniques allow us to study computationally tractable small systems and systematically extrapolate to results for the true infinite system. We find strong numerical evidence that this topologically disordered system is controlled by the same fixed point as the standard Anderson model. While studies interested in the critical exponents have focused on systems close to the localization transition, we are interested in localization lengths across the range of energies and densities relevant to experiments. We use results closest to the critical point to determine two critical parameters and then find localization lengths over the whole system. As we move away from the critical point, corrections to scaling should become more important, and we test our results' sensitivity to these corrections.

The quasi-1D scaling method, originally applied to the standard Anderson model, considers several wires of varying widths w and long lengths [15]. We adapt the recursive Green function version of the scaling technique, introduced by MacKinnon and Kramer, to find the localization length λ_w for equivalent wires in our system [16, 17], see inset to Fig. 1a; other scaling variables may
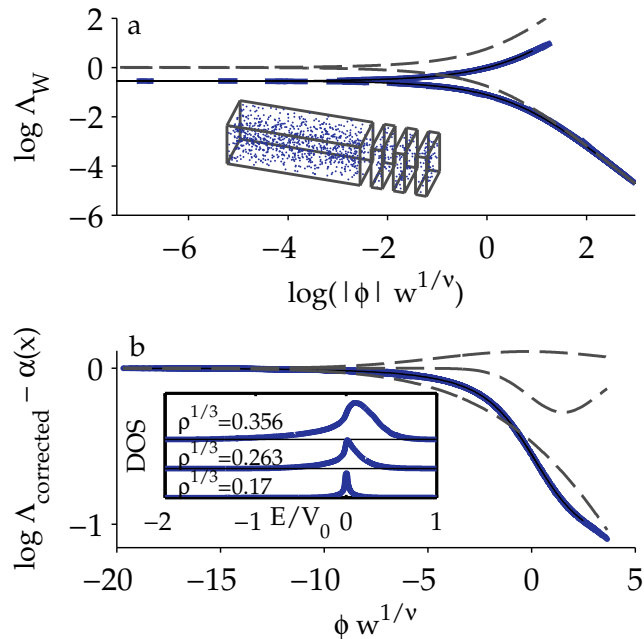
FIG. 1. Scaling function for data with $w \geq 25$, including one correction to scaling η with $y = 2.7$. The thin solid line is the fit. In (a), the dashed line shows the asymptote $\alpha(x) = \nu \sinh^{-1}(x/2)$, showing good agreement in the strongly localized regime (bottom right). In (b), the relevant function $h_0(x)$ minus the asymptotic $\alpha(x)$ is plotted. Dashed lines show the three Gaussians from the fit of δ. Statistical errors in Λ are smaller than point sizes. There are 5829 data points and 893 fit parameters – 8 for the Gaussians, 1 for y, 2 for h_1 and 441 each for $\phi(\rho, E)$ and $\eta(\rho, E)$. The normalized χ^2 statistic per degree of freedom d is 7.5. 70% of the data points are within error of the fit. [Inset in (a)] A wire of width w is constructed by sequentially adding slices (shown at right) to an existing wire. Each slice has length $L_0 \geq L_c$ and has randomly distributed sites of the chosen density. [Inset in (b)] Density of states for three site densities, calculated with 1500 sites and 100 realizations of disorder. Curves offset for clarity. At high density, the DOS becomes asymmetric.

also be considered [18]. The key idea is to divide a long wire into slices, where the sites in each slice are directly coupled only to each other and to sites in the immediately adjacent slices. This is not strictly possible for the system of Eq. 1, as all sites are directly coupled. We take, however, a cutoff L_c and set $\exp(-r/a_B^*) \to 0$ for $r \geq L_c$. We start with a single slice of width w, length $L_0 \geq L_c$ and periodic boundary conditions in two dimensions. We add slices adjacent to the wire and recursively find the portion of the Green function that connects any site in slice 1 to any site in slice N at fixed energy E. We then use the standard method to determine the localization length λ_w of the long wire at energy E [16, 17, 22]. If the width w of any wire is too small, adjacent slices may have no sites within L_c of each other, producing a disconnected wire [24]. Because of the varying number of particles in each slice and the varying off-diagonal matrix

elements, the transfer matrix method (reviewed in Ref. 22) cannot be used.

The statistical error in λ_w can be estimated by assuming that the estimate of λ_w after N slices is the mean of N/λ_w independent and identically distributed samples chosen from a normal distribution, so the sampling error goes down as $N^{-1/2}$ [22]. This is rigorously proved for the standard Anderson model with Oseledec's theorem [22], and we assume that similar statistics hold here. We choose a maximum error of 1%, which requires 10^4 to 10^6 slices, depending on the parameters.

After determining λ_w for a range of widths w, MacKinnon and Kramer (and many others) use the one-parameter scaling theory [25] to extrapolate to infinite size systems. The scaling can be expressed in terms of the relevant variable ϕ, with ϕ greater (less) than zero for extended (localized) states. Then the dimensionless quantity $\Lambda_w \equiv \lambda_w/w$ is a universal function of ϕ and w, with critical exponent ν, [20]

$$\Lambda_w = f[\phi(\rho, E) w^{1/\nu}]. \tag{2}$$

The correlation length is $\xi = |\phi|^{-\nu}$, and we let $\Lambda_c \equiv f(0)$.

If the topologically disordered model is controlled by the same fixed point as the standard Anderson model, then Eq. 2 will hold in our system, with the same $f(x)$. Previous work has expanded $f(x)$ in polynomials [20, 21]. We have not found this to be a successful strategy, at least in part because the underlying functions are strongly nonpolynomial away from the transition region; we know the asymptotic limits $f(x \to \pm\infty) = |x|^{\pm\nu}$ [17]. We choose to fit to $\log \Lambda_w = \log f(\phi w^{1/\nu}) \equiv h_0(\phi w^{1/\nu})$, which must satisfy $h_0(x \to \pm\infty) = \pm\nu \log(\pm x)$. These limits are obeyed by the function $\alpha(x) = \nu \sinh^{-1}(x/2)$. We then fit our data to $h_0(x) = \alpha(x) + \delta(x)$ where $\delta(|x| \to \infty) = 0$.

The scaling form [Eq. 2] applies only for w sufficiently large. At small w, corrections to scaling modify Eq. 2, and they have proven essential for accurate determination of ν and Λ_c [20]. Corrections to scaling require introduction of some number of irrelevant variables $\eta_i(E, \rho)$, which have no effect on the scaling in the limit $w \to \infty$. We illustrate with only one irrelevant variable η. We rewrite our scaling equation as $\log \Lambda_w = h(\phi w^{1/\nu}, \eta w^{-|y|})$, where y is another critical exponent. We expand h in powers of $\eta w^{-|y|}$,

$$\log \Lambda_w = \sum_{m=0} \eta^m w^{-m|y|} h_m(\phi w^{1/\nu}), \tag{3}$$

where h_0 is the limiting one-parameter scaling function. It is often sufficient to keep only $m = 0, 1$ in Eq. 3, [20] which we will do here. We then define $\log \Lambda_{\text{corrected}} \equiv \log \Lambda_w - \eta w^{-|y|} h_1(\phi w^{1/\nu})$.

We are interested in finding the localization length at many values of E, unlike the usual choice of $E = 0$. We choose 14 values of density and 40 values of energy satisfying $-2 \leq E/V_0 \leq 0.5$, focused around the

relevant energies for the metal-insulator transition near $\rho^{1/3} \approx 0.26$. We do not study $E = 0$ because isolated sites always produce eigenvalues with $E = 0$, causing divergences in the Green functions. The density of states (DOS) is shown in the inset of Fig. 1b. The DOS is well-understood in the low-density [3] and high-density, low energy [9, 12] limits. We discard points in the tails of the DOS contributing less than 0.1% of total states, which are known not to obey one-parameter scaling [26]. We take $L_0 = 15a_B^*$ and $L_c = \min[L_0, w/2]$. At each ρ, we take w from $22a_B^*$ in increments of $3a_B^*$ up to the largest system size we find computationally tractable. For the 14 densities, the maximum w/a_B^* studied are $(121, 103, 88, 79, 70, 61, 55, 52, 46, 43, 40, 37, 34, 31)$, from lowest to highest density. Previous studies of mobility edges and critical exponents have performed separate scaling at each E [27]. In this work, all of the data collapse onto a single scaling curve, see Fig. 1, showing universality independent of energy. These calculations used approximately 24 CPU-years of computing time.

We approximate $\delta(x)$ as a sum of three Gaussians with nine free parameters. Within the search loop, for each proposed $\delta(x)$, we find $\phi(\rho, E)$ [and possibly $\eta(\rho, E)$] independently at each value of (ρ, E), giving several hundred additional parameters. It would be preferable to have a functional form for $\phi(\rho, E)$, but we did not find a parametrization that permitted accurate fits. We include only (ρ, E) with at least 4 values of w; the average number of values of w at each (ρ, E) is 15. Where included, we approximate $h_1(x)$ as a second order polynomial with $h_1(0) = 1$, which fixes the scale of η.

Since ν and Λ_c are most sensitive to data near the critical point, we determine them with a restricted data set of 934 points at 105 values of (ρ, E) closest to the critical point. Fitting with corrections to scaling gives $\nu = 1.61(55, 68)$ and $\Lambda_c = 0.577$ $(70, 79)$, where the 95% confidence intervals have been determined by bootstrap resampling [28]. In these fits, the normalized least squares χ^2 is approximately half the number of degrees of freedom (710), which may imply that our error estimates are too large. Previous work has shown that in the standard Anderson model $\nu = 1.58 \pm 0.03$ and $\Lambda_c = 0.576 \pm 0.002$ [20]. Given this confirmation that the critical parameters of the two models agree, the remaining fits are performed with ν and Λ_c fixed to 1.58 and 0.576, respectively [29]. The consistency of Λ_c with previous work indicates that the lattice spacing in the standard Anderson model is equivalent to a_B^* in this model.

Figure 1a shows the scaled data, with one correction to scaling. The upper branch shows the extended states $(\Lambda \to \infty$ as $w \to \infty)$ and the lower branch shows localized states. The extended state curve does not approach its $\phi \to \infty$ asymptote due to a lack of data in the computationally demanding high-density regime. Figure 1b shows the same fit with α and the irrelevant corrections subtracted. The dashed lines show the constituent Gaussians in δ, which are not well-constrained in the fits. See appendix for other fits. Figure 2 shows the resultant correlation length $\xi(\rho, E) = |\phi|^{-\nu}$. At each ρ, the correlation length falls smoothly as E moves away from the delocalization transition, just as we expect. These results give confidence that the $\phi(\rho, E)$ are not simply arbitrary parameters that happen to produce good scaling fits but rather are determined by the underlying physics. We find, however, that $\phi(\rho, E)$ [and thus $\xi(\rho, E)$] is quantitatively determined only for localized states.

Previous high accuracy numerical works on the standard Anderson model have evaluated their fits with the quality of fit Q (also known as the p value) from the χ^2 statistic and the number of fitting parameters N_P [20]. Our fits to the full data have $Q = 0$, indicating that statistical fluctuations of the numerical procedure alone are insufficient to explain the deviations of the data from the model. This is not, however, surprising. Our study has several thousand degrees of freedom, $d = N_D - N_P - 1$, where N_D is the number of data points, which gives it statistical power to detect relatively small deviations between the model and the data. In the true scaling function, $\delta(x)$ is not actually a sum of three Gaussians, and we are sensitive to the deviations between the true $\delta(x)$ and its model. We should be able to add more Gaussians to δ to better approach the universal function, but fitting becomes difficult. If we are not entirely interested in the exact shape of $\delta(x)$, then this deviation is not a concern. We cannot, however, exclude the possibility that the deviation is caused by the scaling procedure breaking down away from the critical point.

Since we are interested in extracting correlation lengths $\xi = |\phi|^{-\nu}$, a better determination of the quality and confidence of the fits is to compare the resultant $\phi(\rho, E)$ for different fitting procedures. We compare fits with and without corrections to scaling and with the smallest w being 22, 25, or 28, in units of a_B^*. Depending on initial guesses, fits can arrive at a number of different local minima. We use a multistart procedure for the fitting, starting with 100 widely varying parameters for $\delta(x)$ and $h_1(x)$. We find that the "best fits," judged solely by minimizing χ^2, have highly oscillatory $\delta(x)$, discontinuous $\phi(\rho, E)$, large deviations from the asymptotic form even for strongly localized states, or large corrections to scaling; they generally have multiple of these features. If we exclude the fits with these four characteristics, for $w \geq 25$ the best fits without (with) corrections to scaling have $\chi^2/d \approx 70$ (8). Including the anomalous fits, we can find $\chi^2/d \approx 31$ (4). We find $\phi(\rho, E)$ from 92 different fits and, independently at each (ρ, E), find the mean $\langle \phi \rangle$ and standard deviation $\Delta\phi$, shown in Fig. 2b. The values of $\phi(\rho, E)$ are found to vary by less than 10% in the localized regime, except for the points closest to the delocalization transition. For $\xi < 100a_B^*$, we can consider the localization lengths to be given quantitatively by the scaling method. Because of the lack of strongly extended
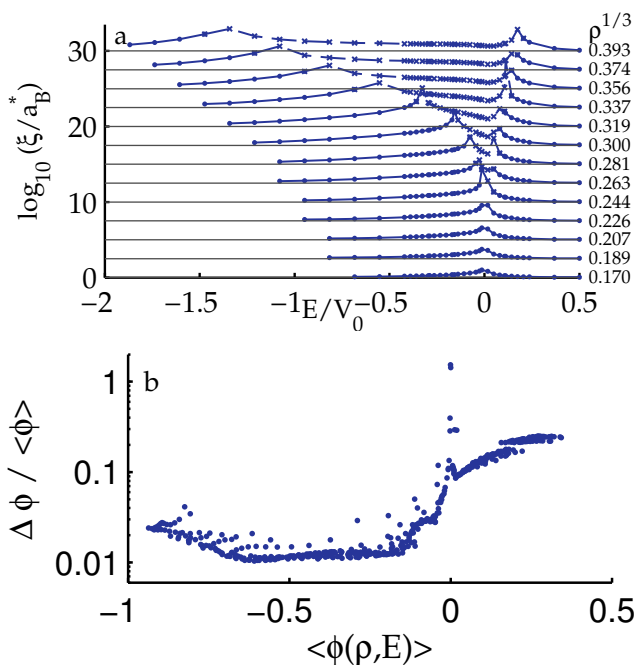
FIG. 2. (a) Correlation lengths $\xi(\rho, E)$ from the fit of Fig. 1, for each of the 13 densities which produced enough data to be studied, offset for clarity. Solid circles mark localized states and crosses mark extended states. Solid and dashed lines are guides to the eye. As expected, the correlation length increases smoothly as the mobility edge is approached from either side. This figure shows the choice of energies for study, which are focused on the area of interest for the critical density, near $\rho^{1/3} = 0.24$. The mobility edge is asymmetric just as is the density of states, with the upper mobility edge closer to $E = 0$ than the lower mobility edge. The (ρ, E) with low density of states (lower left) are excluded. (b) Deviations in fitted values of the scaling variable $\phi(\rho, E)$ from 92 different fits with and without corrections to scaling and with the smallest value of w taken to be 22, 25, or 28 (in units of a_B^*). Localized states with $\phi < -0.05$ are determined within 10% by the scaling fits. See Appendix.

states, $\delta(x > 0)$ is not well-determined, and the fits show a range of different shapes. It follows that $\phi(\rho, E)$ in the delocalized region varies widely. Accumulating more data in the extended regime should fix this problem.

This scaling technique quantitatively gives the localization lengths at nearly any localized (ρ, E) we care to study. Application of this method to systems with on-site disorder, in addition, should shift the mobility edges "inwards" so that more states are localized. These localization lengths allow insight into the properties of a range of material systems, and in future work we will consider their effect on intermediate-band photovoltaics.

[1] P. W. Anderson, Phys. Rev. **109**, 1492 (1958).
[2] P. A. Lee and T. V. Ramakrishnan, Rev. Mod. Phys. **57**, 287 (1985).
[3] A. Amir, Y. Oreg, and Y. Imry, Phys. Rev. Lett. **105**, 070601 (2010).
[4] G. Ambrosetti, I. Balberg, and C. Grimaldi, Phys. Rev. B **82**, 134201 (2010).
[5] O. Mülken and A. Blumen arXiv:1101.2572, p. 29.
[6] A. Luque *et al.*, Physica B **382**, 320 (2006); N. López *et al.*, Phys. Rev. Lett. **106**, 028701 (2011).
[7] M. Morgenstern *et al.*, Phys. Rev. Lett. **89**, 136806 (2002); K. Hashimoto *et al.*, *ibid.* **101**, 256802 (2008); A. Richardella *et al.*, Science **327**, 665 (2010); D. Clément *et al.*, New J. Phys. **8**, 165 (2006); J. Billy *et al.*, Nature **453**, 891 (2008).
[8] I. M. Lifshitz, Soviet Physics Uspekhi **7**, 549 (1965).
[9] T. Matsubara and Y. Toyozawa, Prog. Theor. Phys **26**, 739 (1961).
[10] W. Y. Ching and D. L. Huber, Phys. Rev. B **25**, 1096 (1982); D. E. Logan and P. G. Wolynes, *ibid.* **31**, 2437 (1985); J. Chem. Phys. **85**, 937 (1986).
[11] B. I. Shklovskii and A. L. Efros, *Electronic Properties of Doped Semiconductors* (Springer-Verlag, 1984).
[12] M. Mézard, G. Parisi, and A. Zee, Nucl. Phys. B **559**, 689 (1999).
[13] A. Amir, Y. Oreg, and Y. Imry, Phys. Rev. B **77**, 165207 (2008).
[14] D. J. Priour arXiv:1004.4366.
[15] J. L. Pichard and G. Sarma, J. Phys. C **14**, L127 (1981).
[16] A. MacKinnon and B. Kramer, Phys. Rev. Lett. **47**, 1546 (1981).
[17] A. MacKinnon and B. Kramer, Z. Phys. B **53**, 1 (1983).
[18] B. I. Shklovskii *et al.*, Phys. Rev. B **47**, 11487 (1993).
[19] A. P. MacKinnon, J. Phys.: Condens. Matter **6**, 2511 (1994).
[20] K. Slevin and T. Ohtsuki, Phys. Rev. Lett. **82**, 382 (1999); K. Slevin, P. Markos, and T. Ohtsuki, Phys. Rev. B **67**, 155106 (2003).
[21] A. Rodriguez *et al.*, Phys. Rev. Lett. **105**, 046403 (2010).
[22] P. Markos, Acta Physica Slovaca **56**, 561 (2006).
[23] P. P. Edwards and M. J. Sienko, Phys. Rev. B **17**, 2575 (1978).
[24] J. P. G. Taylor and A. MacKinnon, J. Phys.: Condens. Matter **1**, 9963 (1989).
[25] E. Abrahams *et al.*, Phys. Rev. Lett. **42**, 673 (1979).
[26] L. I. Deych *et al.*, Phys. Rev. B **68**, 174203 (2003).
[27] B. R. Bulka, B. Kramer, and A. MacKinnon, Z. Phys. B **60**, 13 (1985); B. Kramer *et al.*, Physica A **167**, 163 (1990); J. Brndiar and P. Markos, Phys. Rev. B **74**, 153103 (2006).
[28] T. J. DiCiccio and B. Efron, Statist. Sci. **11**, 189 (1996).
[29] Determining ν and Λ_c from the whole data set gives large uncertainty in ν both because the states in the asymptotic region can be fit with nearly any ν and, relatedly, due to the multiple local minima (see main text). The best fits to the full data, including corrections to scaling, have $1.59 \leq \nu \leq 1.85$.

APPENDIX: Scaling curves without corrections to scaling

As discussed in the main text, several fitting procedures can be used to produce plots similar to those in Figs. 1 and 2. We illustrate here that the choice of fitting procedure does not significantly change the localization lengths extracted. Fig. 3 shows fits equivalent to those in Fig. 1, without including corrections to scaling. The scaling still looks very good, though Fig. 3b shows that the data points do not fall on the scaling curve as precisely as in Fig. 1b. The overall shape of the scaling curve deviates from that in Fig. 1 mostly in the extended region, $\phi > 0$, which is not well determined from the data. Additionally, though the overall curve is very similar in shape to that in Fig. 1b, the underlying Gaussians are different, which illustrates the difficulty in converging the fits of $\delta(x)$.

The correlation lengths ξ extracted from these fits are shown in Fig. 4a. They are clearly very similar to those in

FIG. 4. (a) Correlation lengths $\xi(\rho, E)$ from the fit of Fig. 3, for each of the 13 densities which produced enough data to be studied, offset for clarity. Plot is similar to Fig. 2a. Solid circles mark localized states and crosses mark extended states. Solid and dashed lines are guides to the eye. (b) Similar to Fig. 2b, deviations in the fitted values of $\phi(\rho, E)$. Blue points show deviations for 65 fits with no corrections to scaling. Green points show deviations for 27 fits with corrections to scaling. Both include data sets with $w \geq 22$, 25, and 28.

Fig. 2a, showing that the scaling fits robustly determine $\xi(\rho, E)$, regardless of whether corrections to scaling are used. Fig. 2b shows the deviations in the fitted values of ϕ for 92 different fits with and without corrections to scaling.

Fits including corrections to scaling have larger disagreements in $\phi(\rho, E)$. Fig. 4b shows the deviations for 65 fits without corrections to scaling (blue) and 27 fits with corrections to scaling (green). The fits without corrections to scaling have a smaller number of fit parameters, which seems to constrain the fits more. In any of the cases studied, the states with $\xi < 100a_b^*$ are quantitatively determined within 10% by the fits. The consistency of the fits without corrections to scaling argues for use of that method in future studies, despite the large values of χ^2 produced by ignoring the corrections to scaling.
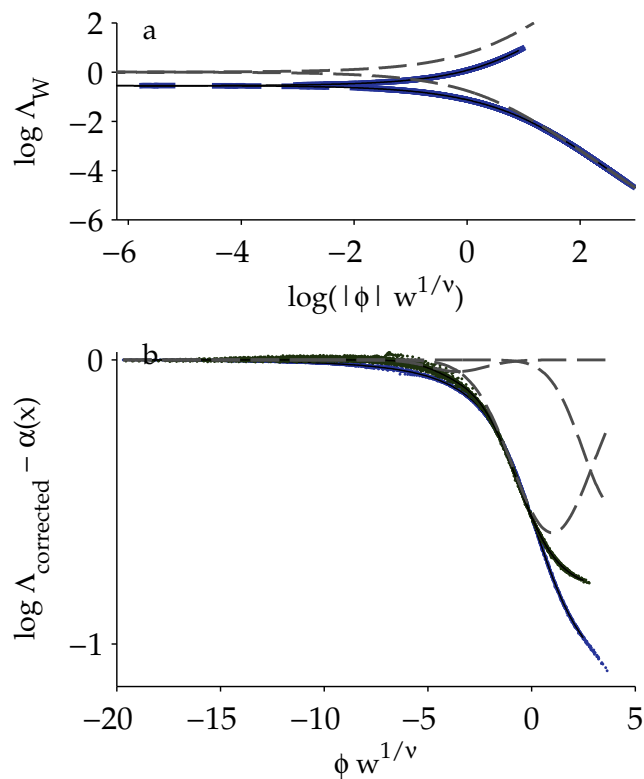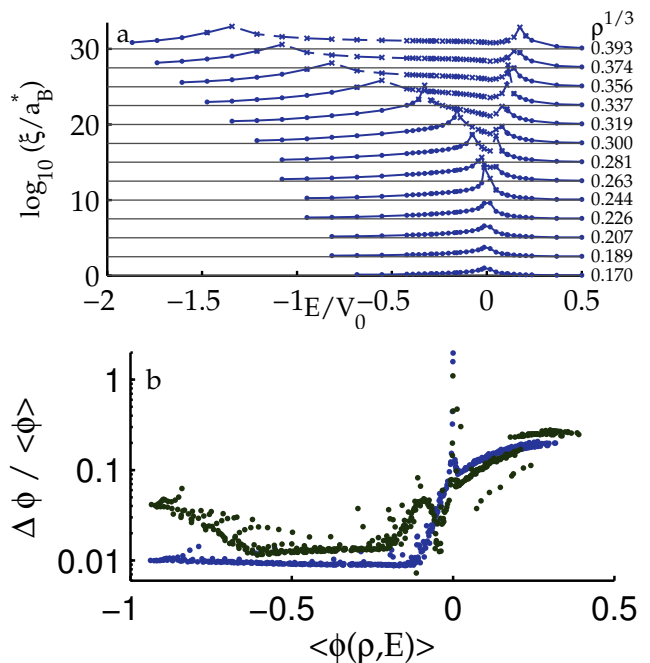

FIG. 3. Scaling function for data with $w \geq 25$, including no corrections to scaling. The scaling is very similar to that in Fig. 1 and produces similar ξ (see Fig. 4a). In (b), blue points are the same as in Fig. 1b while green points are those of the new fit. Dashed lines show the three Gaussians from the new fit of δ, which are clearly different from those in Fig. 1. There are 5829 data points and 449 fit parameters. The normalized χ^2 statistic per degree of freedom d is 71.2. 39% of the data points are within error of the fit.